

### Central European Journal of Physics

# Spectral characterization of hydrogen-like atoms confined by oscillating systems

Research Article

Felix lacob1\*

1 West University of Timişoara, V Pârvan Ave 4, 300223 Timişoara, Romania

#### Received 28 November 2013; accepted 26 May 2014

Abstract: The spectral characterization of Coulomb systems confined by a homogeneous pseudo-Gaussian oscillator

is investigated. This is done using the efficient computational method of generating functionals. Also, this method is used for the spectral characterization of homogeneous harmonic oscillator confinement, treated as a particular case of pseudo-Gaussian oscillator confinement. Finally, confinement by an impenetrable sphere of finite radius is considered by studying its conjugate effect along with a harmonic oscillator.

PACS (2008): 02.70.-c; 02.70.Hm; 03.65.Ge

**Keywords:** Hamiltonian system • generating functional method • energy spectrum

© Versita sp. z o.o.

### 1. Introduction

Coulomb systems are still of interest in literature and are used as a model in many domains of applied physics. Atomic physics is an extensive domain, where soft-core (truncated) Coulomb systems are used to describe the interaction of intense laser fields with atoms [1, 2]. Models of hydrogen-like atoms in different confinement situations are used to simulate the effect of high pressure on atomic static dipole polarizability. One of these models, known as hard confinement, is an impenetrable sphere of finite radius confining the atom [3]. Sommerfeld and Welkerto obtained the wave function solution in terms of confluent hypergeometric functions and emphasized that this model can be used to predict the line spectrum of hydrogen-like

atoms in the outer atmosphere [4]. Soft confinement of Coulomb systems was introduced by superimposing Debye screening [5]. This leads to the idea of using the harmonic oscillator (HO) for atom confinement, known as the soft wall confinement (SWC) model. The asymptotic iteration method (AIM) was used [6] for the spectral characterization of a spherically confined  $-a/r + br^2$  potential. In one of his papers, studying the Zeeman effect, Avron [7] considered a Hamiltonian in which the Zeeman potential in a uniform magnetic field is replaced by the rotationally symmetric one  $V \propto r^2$ . Using WKB technigues, he derived the large-order behavior of the perturbation series for all energy levels. The large-order behavior of the SWC system was also studied by Janke and Kleinert [8], exploiting the idea that the Coulomb system in three dimensions can be mapped onto an oscillator system in four dimensions, and this was done using the Bender-Wu formulas. Recently, the physical model of the pseudo-Gaussian oscillator (PGO) was introduced in [9]

<sup>\*</sup>E-mail: felix@physics.uvt.ro

for Schrödinger and in [10] for Klein-Gordon systems, and the energy levels were determined using the generating functional method (GFM). The PGO potentials have HO properties approaching zero and include the genuine HO potential as a limit. It is well known that the HO potential has an infinite number of equidistant energy levels; however, PGO potentials have a finite number of energy levels and the interval between two consecutive levels increases slightly on higher levels. The GFM is a computational method developed to solve the eigenvalue problem by integration and to evaluate the expectation values for energy levels of physical systems through successive differentiation. This is an accurate method which works well for systems with a finite number of energy levels.

One aspect we would like to present in this paper is the spectral characterization of the atom spherically confined by the pseudo-Gaussian oscillator, using the GFM. We will say this is a finite soft wall confinement (FSWC) model. Also, the energy spectra for SWC, found as a particular case of FSWC, is evaluated with the same technique, and the data values obtained are compared with those in the literature. Another aspect we would like to present is how the energy level values of the SWC system vary when introducing confinement by an impenetrable sphere of finite radius. We will show that the degeneracy of energy states for a free atom are lifted in the case of confinement.

The original inspiration for confinement came from atoms under extreme pressure and heat. Another example is the atom within a solid, where the idea is that an atom confined in a Wigner-Seitz cell might develop a conduction band. If we retain this idea, then the process by which the electron becomes "free" should perhaps be described as "delocalisation" rather than ionization. This arises when the ground state energy of the confined atom rises above the ionization threshold of the free atom. Considering this, we propose this PGO confinement model for a better understanding of both the atom under extreme pressure and heat and metal-insulator transitions, by providing energy values for an electron in such perturbed atoms. PGO can also be used as a confinement model in the behavior of novel nano-structures such as quantum dots, quantum wires and other micro-electronic devices [11]. As mentioned above, the PGO model admits a finite number of energy levels. These levels can be manipulated by choosing a numerical value for the reference energy  $\lambda$  which sets the depth of the potential well. From this point of view, this PGO confined model is actually closer to reality for these nano-devices.

Over time, other computational and approximate mathematical methods have been developed and used to solve the eigenvalue problem of the Schrödinger equation with

different types of potentials which cannot be analytically solved. Let us mention some of them: the variational method [12], the functional analysis method [13], the supersymmetric approach [14], the asymptotic iteration method [15], and the factorization method [16]. Also, there are other known adapted methods to the various cases of exact quantization [17, 18].

The paper is organized as follows: Section (2) is dedicated to the physical model with a review of the pseudo-Gaussian potential, Section (3) provides a brief exposure to the standard GFM, Section (4) shows how the GFM works for the physical model considered here and Section (5) presents the calculated spectral characterization results for atom confinement.

## 2. The physical model

Let us consider the radial part of the three-dimensional Schrödinger time-independent equation  $H\psi=E\psi$ . The Hamiltonian H, given in atomic units,

$$H = -\frac{1}{2}\Delta + V(r),\tag{1}$$

introduces the potential V(r):

$$V(r) = -\frac{1}{r} + W_{\lambda,\mu}^{s}(r), \tag{2}$$

where, for confinement, the pseudo-Gaussian potential,  $W^s_{\lambda,\nu}(r)$  is added to the hydrogen atom potential

$$W_{\lambda,\mu}^{s}(r) = \left(\lambda + \sum_{k=1}^{s} C_k r^{2k}\right) \exp(-\mu r^2), \tag{3}$$

with the coefficients  $C_k$  defined as

$$C_k = \frac{(\lambda + k)\mu^k}{k!} \,. \tag{4}$$

The properties of these models are completely determined by the dimensionless parameters  $\mu$ ,  $\lambda \in \mathbb{R}$  and the positive integer s=1,2,... which is called the order of the PGO. We note that the genuine Gaussian potential corresponding to s=0 is not included in this family. The potentials defined by Eqs. (3) and (4) have the remarkable property that they approach the potential of the HO when  $r\to 0$ . Moreover, it can be proved that for each order s, the Taylor expansion of these potentials,

$$W_{\lambda,\mu}^{s}(r) = \lambda + \mu r^2 + O(r^{2s+2}),$$
 (5)

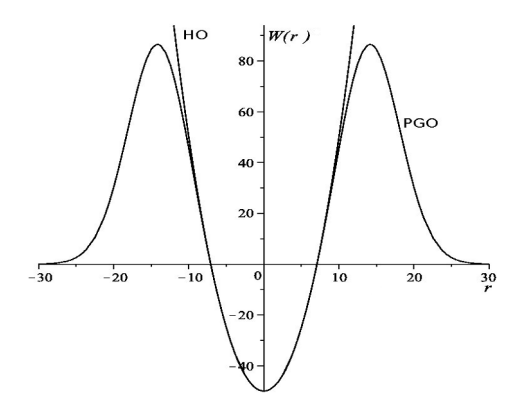


Figure 1. The pseudo-Gaussian oscillator potential graph compared with harmonic oscillator potential one.

does not include terms proportional to  $r^4$ ,  $r^6$ , ...,  $r^{2s}$ . Therefore, when s increases, the potential (3) is approaching that of the HO and the potential (2) becomes:

$$V(r) = -\frac{1}{r} + \frac{1}{2}\hat{\omega}^2 r^2 \tag{6}$$

with centrifugal constant  $\hat{\omega}=\sqrt{2\mu}$  measuring the strength of confinement. In Figure (1), the graphs of both the PGO and HO are shown to illustrate their similar shapes in the vicinity of the origin.

Taking into consideration that l(l + 1) represents the eigenvalue of the square of the angular-momentum operator, the radial part of H can be written explicitly as:

$$-\frac{1}{2}\left(\frac{d^2}{dr^2} + \frac{2}{r}\frac{d}{dr} - \frac{l(l+1)}{2r^2}\right) + V(r),\tag{7}$$

and with the potential (2) we can study the radial three dimensional Schrödinger eigenvalue problem for the pseudo-Gaussian potential confinement, i.e. the FSWC model. In the particular case of SWC, the potential (6) is used in the Hamiltonian (7), so we get the radial three dimensional Schrödinger eigenvalue problem for HO confinement.

## 3. The generating functional method

To apply the GFM to this model, it is necessary to specify a basis for the Hilbert space of states. Considering hydrogen atoms in different confinement situations, it is suitable to make use of their radial wave-functions as a canonical basis for the Hilbert space. The radial functions, solutions to the Schrödinger time-independent equation

for hydrogen-like atoms, are given in terms of Laguerre polynomials by:

$$R_{n,l}(r) = -\frac{2}{n^2} \sqrt{\frac{(n-l-1)!}{(n+l)!}} e^{-\frac{r}{n}} \left(\frac{2r}{n}\right)^l L_{n-l-1}^{2l+1} \left(\frac{2r}{n}\right).$$
(8)

The generalized Laguerre polynomials may be written with the help of a generating function and according to [24] are:

$$L_p^a(x) = \frac{1}{p!} \frac{\partial^p}{\partial \sigma^p} (1 - \sigma)^{-a-1} e^{\frac{x\sigma}{\sigma-1}} \bigg|_{\sigma=0} ,$$

where in our case x is replaced with  $\left(\frac{2r}{n}\right)$ , p with n-l-1 and a with 2l+1, with n and l the well known principal and orbital quantum numbers.

For any radial operator  $\mathcal{X}$ , we can calculate the generating functional as:

$$Z(\tau,\sigma)[\mathcal{X}] = \int_0^\infty dr \ r^2 \ R_{n',l}(r) [\mathcal{X}R_{n,l}](r) , \qquad (9)$$

The matrix elements of the operator  $\mathcal{X}$ , can be derived from the generating functional (9) as follows:

$$\langle n' l' | \mathcal{X} | n l \rangle = \delta_{l', l} \left. \frac{1}{n'! n!} \partial_{\sigma}^{n'} \partial_{\tau}^{n} Z(\sigma, \tau) [\mathcal{X}] \right|_{\sigma = \tau = 0}. \quad (10)$$

For spectral characterization,  $\mathcal{X}$  is replaced with the specific Hamiltonian operator.

The physical problem of studying the atom in different confinement situations allows us to view the Hamiltonian (7) as made up by the part  $H_a = -\frac{1}{2}\Delta_r - \frac{1}{r}$  describing the atom and the perturbative part  $H_i = W_{\lambda,\mu}^s(r)$  describing the confinement. This approach can be found in the literature, for example in Ref. [22]. This justifies the choice made at the beginning of this section to calculate the generating functional (9) in the canonical basis of atom (8) using Laguerre polynomials. The generating functional is rewritten as:

$$Z(\tau,\sigma)[H] = Z(\tau,\sigma)[H_a] + Z(\tau,\sigma)[H_i], \tag{11}$$

so the energy levels of the system are corrective to those of the atom and follows from

$$\langle n' l' | H | n l \rangle = \delta_{l',l} \frac{1}{n'! n!} \left[ \partial_{\sigma}^{n'} \partial_{\tau}^{n} Z(\sigma, \tau) [H_{\sigma}] + \partial_{\sigma}^{n'} \partial_{\tau}^{n} Z(\sigma, \tau) [H_{l}] \right]_{\sigma=\tau=0}^{l},$$
(12)

In the computation process, N steps of differentiation have been taken, so we obtain an  $(N\times N)$  matrix which in general is not a diagonal one, due to the perturbative term. To obtain the values of the energy levels, the matrix (12) will be subject to a diagonalization process. The effective calculation of generating functional (11) is made by solving the integrals appearing in the kinetic part  $Z(\tau,\sigma)[-\frac{1}{2}\Delta]$  as well as in the potential part  $Z(\tau,\sigma)[r^{-1}]$  along with  $Z(\tau,\sigma)[W^s_{\lambda,\mu}(r)]$ . This will be presented in the following section.

# 4. The generating functional in the case of hydrogen-like atom confinement

In the case of potential (2), the GF (11) can be organized as a sum of terms:

$$Z(\tau, \sigma)[H] = Z(\tau, \sigma) \left[ -\frac{1}{2} \Delta \right] + Z(\tau, \sigma) \left[ r^{-1} \right]$$

$$+ Z(\tau, \sigma) \left[ W_{\lambda,\mu}^{s}(r) \right].$$
(13)

In the evaluation process, the advantage of this method is that the integrals (13) reduce to known Gaussian ones. To do so, we have to specify the shape of the potential, *i.e.*, to give the order s and the coefficients  $\mu$  and  $\lambda$ . In this paper, our computations are made with potentials of order s=3, a case in which the potential (5) expands as

$$W_{\lambda,\mu}^{s=3}(r) = \lambda + \mu r^2 + (14)$$

$$\left(-\frac{1}{6} - \frac{\lambda}{24}\right) \mu^4 r^8 + \left(\frac{1}{8} - \frac{\lambda}{30}\right) \mu^5 r^{10} + \left(-\frac{1}{20} - \frac{11\lambda}{720}\right) \mu^6 r^{12} + \left(\frac{1}{80} - \frac{\lambda}{360}\right) \mu^7 r^{14} + \dots$$

Having the explicit form of potential  $W_{\lambda,\mu}^{s=3}(r)$ , it is observed that the GF (13) consists of a sum of terms containing different powers of r,

$$Z(\tau, \sigma)[H] = \sum_{k} Z_{k}(\tau, \sigma) [r^{k}],$$

$$k = \{-1, 0, 2, 8, 10, 12, ...\}$$
(15)

with the calculated terms

$$Z(\tau, \sigma) \left[ r^{k} \right] = 2^{2l+1} (nn')^{l+k+1}$$

$$\times \sqrt{\frac{(n-l-1)!(n'-l-1)!}{(n+l)!(n'+l)!}}$$

$$\times \frac{(2l+k+2)! \left[ (1-\sigma)(1-\tau) \right]^{k+1}}{\left[ (n+n')(1-\sigma\tau) + (n'-n)(\sigma-\tau) \right]^{2l+k+3}},$$
(16)

where k takes the value  $\{0\}$  for the kinetic part, the first term in (13);  $\{-1\}$  for the atom part, the second term in (13);  $\{2\}$  for the HO part from the pseudo-Gaussian potential (14); and  $\{8,10,12,\ldots\}$  for the next terms with higher power coming from the pseudo-Gaussian potential expansion (14). In the case when  $s \to \infty$ , the potential (2) tends to the potential (6) whereupon the GF (15) is stripped of the higher power terms and becomes

$$Z(\tau, \sigma)[H] = Z(\tau, \sigma) \left[ -\frac{1}{2} \Delta \right] + Z(\tau, \sigma) \left[ r^{-1} \right]$$

$$+ \frac{1}{2} \hat{\omega}^2 Z(\tau, \sigma) \left[ r^2 \right],$$
(17)

the GF for the SWC.

### 5. Numerical results

The energy values  $\varepsilon_n$  are obtained using the matrix elements given by

$$\varepsilon_n = \delta_{l',l} \left. \frac{1}{n!^2} \mathcal{D}iag \left[ \partial_{\sigma}^n \partial_{\tau}^n \sum_k Z(\tau,\sigma)[r^k] \right|_{\sigma=\tau=0} \right], \quad (18)$$

where  $\mathcal{D}iag$  stands for the diagonalization procedure of the matrix. First, the code was tested in the particular case of the hydrogen atom where the generating functional (15) is:

$$Z(\tau,\sigma)[H_{\sigma}] = \frac{1}{2n'^2} \left(\frac{1+\sigma}{1-\tau}\right)^2 - \left[1 + \frac{\tau+1}{n'} \frac{1+\sigma}{1-\tau}\right].$$
(19)

The numerical values of energy, calculated with (18), respect the known analytical relation  $\varepsilon_n = -\frac{1}{n^2}$  so  $E_n =$  $\varepsilon_n E_0$  with  $E_0 = 13.6 \, ev \, (n = 1, 2 \ldots)$ . This confirms that the code is working properly and the values have been exactly retrieved, as they are known values. Next, we have added the pseudo-Gaussian potential in the code to determine the energy spectrum for the FSWC. The calculated numerical values of energy are presented in Figure (2). The levels up to a critical number are negative, known as bound states, and the rest are positive. In other words, the energy spectrum of the confined atom does not belong entirely to the negative domain, as happens in the case of the free atom. We can say that, after the ionization of the atom, the electrons can take only a certain amount of energy. This seems to be reasonable in the case of confinement—discrete spectra with positive energies were also reported in the literature (one may consult [3, 4]). Furthermore, an inflection point is observed at the boundary between the negative and positive domains of

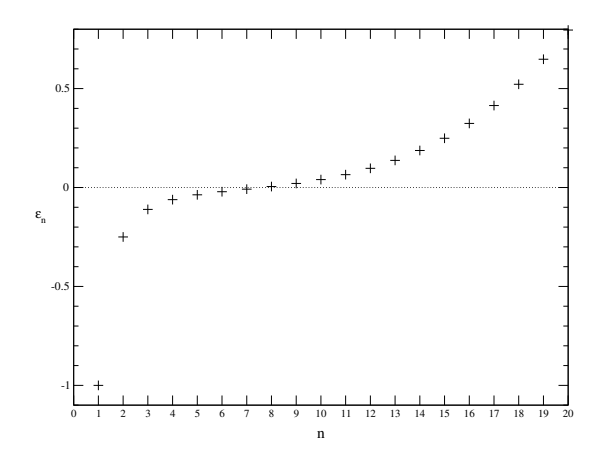


**Figure 2.** The calculated energies  $\varepsilon_n$  of a PGO confined atom, with  $s=3,\,\mu=2\times 10^{-10}$  and N=20.

energy levels. This occurs because the first energy levels are near the nucleus of the atom and are controlled by the Coulomb part of the potential. Moving away from the nucleus, the PGO potential becomes dominant and the levels become more distant from each other. The number of energetic values depends on the strength of confinement, so changing  $\mu$  changes the number of negative energetic values. Also, changing s changes the number of positive energetic values.

The eigenstates with positive eigenvalues are meta-stable states. A particle that is bound by some attractive force is able to escape even if it lacks the energy to overcome the attractive force. Classical physics predicts that such behavior is impossible. However, the fuzziness of nature at the sub-atomic scale, inherent in quantum mechanics, implies we cannot know precisely the trajectory of a particle; this uncertainty means the particle has a small but nonzero probability of suddenly finding itself outside. We say it has tunneled through a potential energy barrier created by the attractive force. The shape of the PGO potential, Figure (1), appears like a well bordered by barriers. Thus, this potential admits eigenstates with positive energies, known as meta-stable states or resonances.

The transmission amplitude T of these meta-stable states through the bordering barriers can be estimated with the help of the transfer matrix M on a finite domain. An extensive presentation of the transfer matrix method is provided in [19]. Roughly speaking, the idea is that one can consider a barrier potential made of successive narrow constant barriers. In this way we express the transfer matrix M as a product of matrices  $M_i$ . Each  $M_i$  characterizes the effect of individual discontinuities of the "i-th" sector and so the propagation through the entire discretized structure is  $M = \prod_i M_i$  taken in the proper order. The transmission amplitude expressed in terms of the transfer matrix can be

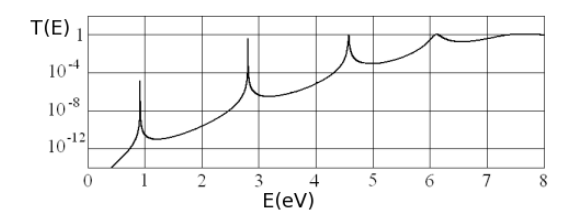


Figure 3. The calculated transmission amplitude of PGO [9].

written as [20]:  $T = \frac{1}{|\mathcal{M}_{11}|^2} \tag{20} \label{eq:20}$ 

A peak of the transmission amplitude corresponds to a resonant eigenstate [21]. In accordance with [9], four resonant states are found for the potential shape (s=3) under consideration, corresponding to the four peaks as shown in Figure (3). Thus, the positive spectrum of the FSWC system consists of four resonant states overlapping the continuous spectrum of energies. In an approach that computes the wave functions, it is possible to predict the resonances' life time.

As the numerical data is not so accurate, by reading Figure (2), we give the values of the energy levels, expressed in atomic units, in Table (1). We observe that the values for the first energy levels, closer to the nucleus, in the case of confinement do not differ very much from the first levels of the free atom. The difference between these values becomes apparent only for levels distant from the nucleus. As one can observe, by confinement, the outside levels are energetically more affected.

Table (1) also presents the calculated numerical data for HO confinement and PGO confinement with s=18. As we mentioned above, parameter s measures the closeness of the PGO potential to the HO potential. As one can see, the numerical data are closer to the HO data for s = 18than for s = 3, but this trend is not very pronounced and hardly visible. To see how the atom behaves in transition from the PGO to HO confinement, calculations were made by taking higher orders of PGO. Because the values modify slightly with s, we will present directly the numerical results for HO confinement as the limit of the PGO confinement when s equals infinity by means of a limit process. We will use the same technique to calculate the energies  $\varepsilon_n$ , for this potential, having now  $\hat{\omega}$  as a measure of confinement strength. The behavior of energy levels for some values of  $\hat{\omega}$  are represented graphically as a function of quantum number n in Figure (4). The numerical data values in the case of  $\hat{\omega} = 10^{-6}$  are also given in Table (1). We have compared these data with those obtained by Janke and Kleinert; following the re-

Table 1. The perturbed energy level corrections for a free atom with PGO and HO confinement, in (a.u.).

n	Free atom	PGO confinement	PGO confinement	
		s=3	s=18	$\omega = 10^{-6}$
1	-1.000000	-0.999994	-0.999994	-0.999997
2	-0.250000	-0.249916	-0.249916	-0.249958
3	-0.111111	-0.110697	-0.110697	-0.110904
4	-0.062500	-0.061204	-0.061204	-0.061852
5	-0.040000	-0.036850	-0.036850	-0.038425
6	-0.027778	-0.021262	-0.021262	-0.024520
7	-0.020408	-0.008354	-0.008354	-0.014381
8	-0.015625	0.004919	0.004919	-0.005353
9	-0.012346	0.020540	0.020540	0.004097
10	-0.010000	0.040100	0.040100	0.015050
11	-0.008264	0.065062	0.065062	0.028399
12	-0.006944	0.096880	0.096879	0.044968
13	-0.005917	0.137057	0.137056	0.065570
14	-0.005102	0.187174	0.187172	0.091036
15	-0.004444	0.248906	0.248897	0.122231
16	-0.003906	0.324030	0.323999	0.160062
17	-0.003460	0.414433	0.414335	0.205487
18	-0.003086	0.522114	0.521829	0.259516
19	-0.002770	0.649180	0.648406	0.323213
20	-0.002500	0.797828	0.795860	0.397700

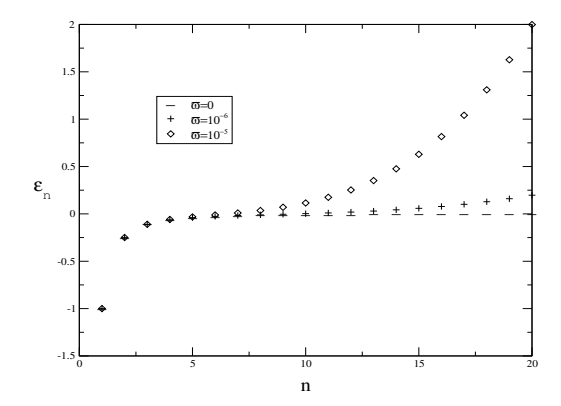


**Figure 4.** The calculated energies  $\varepsilon_n$  for  $\hat{\omega} = \{0, 10^{-5}, 10^{-6}\}.$ 

lation (33) for the energy from their paper [8], we have found that our work is the case p=2 and  $D^C=3$ . The calculated perturbation coefficients, Table (III) from their work, give energies with values comparable to those presented here in Table (1), HO column. However, a slight difference between the values for higher levels is found. We think this happens due to the evaluation process of energies. We give the energies as calculated elements of a diagonalized matrix while they give the energies from a calculation based upon large order behavior of the per-

turbation series. In Figure (4), the energy levels for the atom are also represented by dashed lines. This is the case of no confinement ( $\hat{\omega}=0$ ) and as it is observed, the values of energy levels remain below zero.

Next we ask at what confinement strength magnitude the negative energies disappear. It was found that for  $\hat{\omega} = 1/3$ and above there are no negative energies. This case is presented in Figure (5), and one may say there is a value for  $\hat{\omega}$  above which the atom influence is missing. Let us denote this with  $\hat{\omega}_c$  and consider this as the critical value which accomplishes the condition of positive energies,  $\varepsilon > 0$  for all  $\hat{\omega} > \hat{\omega}_c$ . The numerical values of  $\hat{\omega}_c$ are found to be high for ground state, in comparison with other energy levels. As mentioned above, for the lowest orbital 1s (n = 1, l = 0) the calculated critical value is  $\hat{\omega}_c = 1/3$ . This result is in concordance with the one obtained in Ref. [6] where an analogous value of  $\hat{\omega}_c$ , denoted by  $b_c$  was calculated using an asymptotic iteration method with the value  $b_c = 0.32533$ . The calculated critical values for orbitals  $\{1s, \dots 4f\}$  are presented in Table (2). The range of the critical values is upper-bounded by the one corresponding to orbital 1s and values decrease, as calculations show, for higher orbitals.

In a confined system, it is interesting to investigate the aspect of degeneracy of the energy. To do this, the intensity of confinement is controlled by varying  $\hat{\omega}$ ; starting

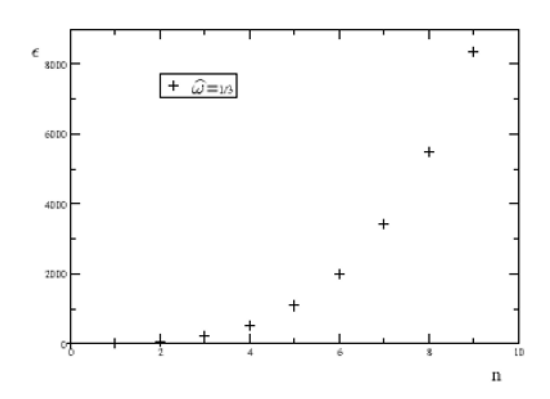


**Figure 5.**  $\hat{\omega} = 1/3$  means positive energy only.

**Table 2.** Critical values for  $\hat{\omega}_c$  above which all energies are positive.

orbital	4f	4d	4p	4s	3d
$\hat{\omega}_c$	0.000173	0.000125	0.000105	0.000097	0.000882
$b_c$	0.00015	0.00010	0.00008	0.00007	0.00079
orbital	25	2	2	2	
o. betat	3р	3s	2р	2s	1s
$\hat{\omega}_c$	'		2p 0.008334		1s 1/3

from the free atom ( $\hat{\omega}=0$ ), the effect of finite  $\hat{\omega}$  is to remove the accidental degeneracy and raise the energy levels. The orbitals  $4s\,4p\,4d\,4f$  were considered to see how degeneracy is removed with  $\hat{\omega}$  and the results are presented in Figure (6). At small values of  $\hat{\omega}$ , the energies of the orbitals are almost identical—this is the free atom case; further increase of  $\hat{\omega}$  by a small amount has as consequences the separation of energy levels of or-

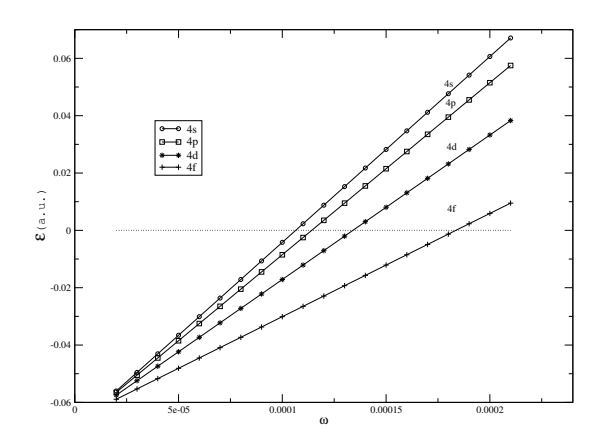


Figure 6. The degeneracy is removed as shown for the orbitals 4s4p4d4f.

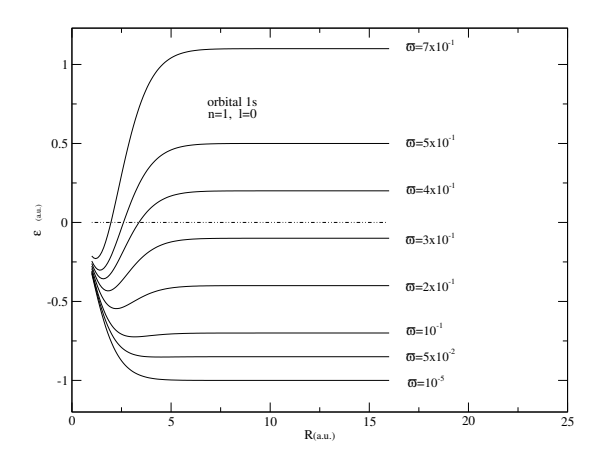
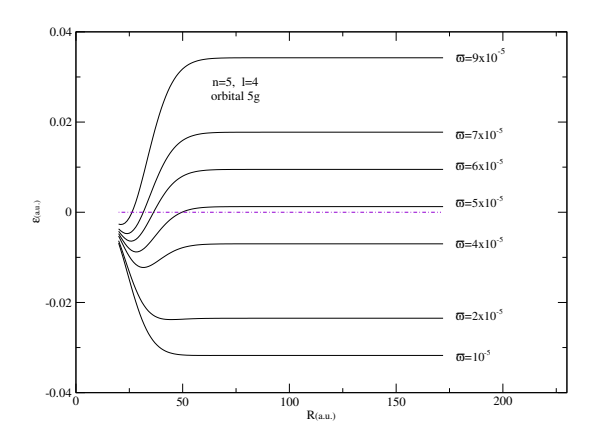


Figure 7. Energy dependence of orbital 1s with both types of confinement.

bitals. Thus for fixed n, the higher l is, the smaller the corresponding energy is. In other words, the states get relatively less destabilized.

Let us consider the confinement of an impenetrable sphere (hard confinement) of finite radius R of the system (1) with the potential (6). Mathematically, hard confinement means that the integrals from relation (16) will be made on a domain bounded by a sphere with radius  $R_i$ , but not smaller than one atomic radius, R > 1. To see how hard confinement affects the states of atom confined by the HO system, the radius R will range and  $\hat{\omega}$  will be taken as a parameter. Our calculations have been performed on the ground energy level, the orbital 1s and the orbital 5g. The behavior of the energy of orbital 1s is presented in Figure (7), with  $\hat{\omega}$  taking values in the set  $\{10^{-5},\,5\times10^{-2},\,10^{-1},\,2\times10^{-1},\,3\times10^{-1},\,4\times10^{-1},\,5\times10^{-1},\,10^{-1},$  $10^{-1}$ ,  $7 \times 10^{-1}$  }. Let us notice that we can divide the domain of values of R into three regions according to how confinement affects energy. The first region, as Rincreases, is in a vicinity of R = 1a.u. where the sphere is very close to the atom. This annihilates the vibrational movement due to HO confinement, so the energy levels do not depend on  $\hat{\omega}$  and the value of energy is  $\varepsilon \approx -\frac{1}{4}a.u.$ , which represents the equivalent of the second energy level (n = 2) for the free atom. The second region follows immediately and ranges until a threshold value  $R_h = 5 a.u.$ This is the region where both types of confinement are explicit. The third region ranges beyond the threshold value  $R > R_h$ . Here, the effect of hard confinement is weak, so the energy remains almost constant. Let us discuss in detail what occurs in the second region. For relatively small  $\hat{\omega} \approx 10^{-5}$ , this is a weak SWC, it is observed that as Ris increased the energy goes down and stabilizes around the value of free atom, i.e.  $\varepsilon \approx -1a.u.$  This is quite well because in this conditions the atom is almost free. It is



**Figure 8.** Energy dependence of orbital 5*g* with both types of confinement

interesting to see the effect of conjugate action for both types of confinement for values of  $\hat{\omega}\approx 10^{-1}$ . One can see in figure (7) that the energy as function of radius of sphere presents a minimum. This behavior does not exist for the side values of  $\hat{\omega}\approx 10^{-5}$  and  $\hat{\omega}\approx 7\times 10^{-1}$ , so it seems there is a resonant region,  $\hat{\omega}\in[5\times 10^{-2},\,5\times 10^{-1}]$ , where the two types of confinement, somehow, annihilate each other and the energy tends to decrease towards the free atom one.

The behavior of energy of orbital 5g is presented in Figure (8). At first glance, the results presented in Figures (7) and (8) look similar: the shape of the energy as a function of sphere radius is preserved and we also have the same three regions. A closer look indicates that the value ranges of R,  $\hat{\omega}$  and the energy values  $\varepsilon$  are different. The first region is in a vicinity of R=25a.u; this value is sufficient for hard confinement to annihilate the SWC for this external energy level. The resonant region of conjugate action extends up to a threshold value of  $R_h=50~a.u$ . and the value for SWC falls to  $\hat{\omega}\approx 10^{-5}$ . This is normal because the exterior orbitals are supposed to be affected much more by confinement than the inner ones.

It has been shown in the literature that, in a confined system, a state with angular momentum (l+1) is more strongly bound than one with l, which is vice versa from the aufbau principle corresponding to a free atom. Taking into consideration the property of monotonicity of the range of energies, it is possible to give rise to crossing pairs of states (n,l) and (n',l') with n'>n, l'>l. Our computation, made in the resonant region of  $\hat{\omega}\approx 10^{-5}$ , shows the existence of crossing states and the results are presented in Figure (9).

In this work, we have obtained novel results about the spectral characterization of perturbed hydrogen-like atoms. We have introduced the PGO as an oscillating

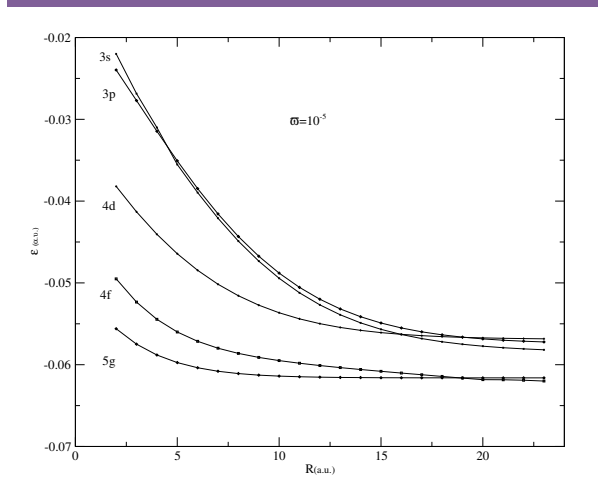


**Figure 9.** Crossing energy states: The level 4*d* is observed crossing 3*d* and 3*s*. Also, 5*g* crosses 4*f*.

system to confine the atom. This allows the existence of discrete positive energy spectra for the system. The existence of an inflection point between the negative and positive energy levels was indicated, and the critical value  $\hat{\omega}_c$  was calculated for each orbital from 1s to 4f. It was shown that in the case of confinement, the accidental degeneracy of the free atom is removed and also the energy increases as strength of confinement is increased. On the other hand, orbitals with the same n are relatively less destabilized as l increases. The effects of conjugate action of hard confinement together with HO upon the atom energy levels were studied. We found that the energy levels as a function of sphere radius have a minimum given by a resonant action of both types of confinement. Finally, the crossing pair of energy states is calculated—they appear due to confinement and apparently are in contrast with the aufbau principle corresponding to the neutral free atom.

We consider this model to be useful in the explanation of the metal-insulator transition (MIT), also called the Mott transition. An atom in an insulator material is subjected to external excitations which are modeled as an oscillating system confinement and which may cause atom ionization and raising of the electron to the conduction band. This effect produces a spontaneous transition from insulator to metal by means of the flow of an electrical current. The electrical conductivity of FeO as a function of pressure and temperature was recently measured ([23]). Although insulating as expected under ambient conditions, it was found that FeO metalizes at high temperatures. Electrical conductivity of FeO was measured up to 141 GPa and 2480 K in a laser-heated diamond-anvil cell.

### **Acknowledgments**

I would like to thank Ion Cotăescu for helpful suggestions, and comments that have improved the development of this paper.

### References

- [1] C.A.S. Lima, L.C.M. Miranda, Phys. Rev. A 23, 3335 (1981)
- [2] Y.I. Salamin, S.H. Hu, K.Z. Hatsagortsyan, C.H. Keitel, Phys. Rep. 427, 41 (2006)
- [3] A. Michels, J. de Boer, A. Bijl, Physica 4, 981 (1937)
- [4] A. Sommerfeld, H. Welker, Ann. Physik 32, 56 (1938)
- [5] J.C. Stewart, K.D. Pyatt , Phys. Rev. 144, 1203 (1966)
- [6] R.L. Hall, N. Saad, K.D. Sen, J. Phys. A: Math. Theor. 44, 185307 (2011)
- [7] J.E. Avron, Ann. Phys. (NY) 131, 73 (1981)
- [8] W. Janke, H. Kleinert, Phys. Rev. A 42, 2792 (1990)
- [9] I.I. Cotaescu, P. Gravila, M. Paulescu, Int. J. Mod. Phys. C 19, 1607 (2008)
- [10] F. Iacob, Phys. Lett. A 374, 1332 (2010)
- [11] S. Titus, Aplicatii ale inteligentei artificiale in domeniul economicsi tehnic (Mirton Publishing House, Timisoara, 2007)
- [12] B. Batiha, Aus. J. Basic Appl. Sci. 3, 3876 (2009)

- [13] Y. Zhang, Phys. Scr. 78, 015006 (2008)
- [14] G. Chen, Z.-D. Chen, Z.-M. Lou, Phys. Lett. A 331, 374 (2004)
- [15] H. Ciftci, R.L. Hall, N. Saad, J. Phys. A: Math. Gen. 36, 11807 (2003)
- [16] S.-H. Dong, Factorization Method in Quantum Mechanics (Springer, Netherlands, 2007)
- [17] Z.-O. Ma, A. Gonzales-Cisneros, B.-W. Xu, S.-H. Donq, Phys. Lett. A 371, 180 (2007)
- [18] X.-Y. Gu, S.-H. Dong, Z.-Q. Ma, J. Phys. A: Math. Theor. 42, 035303 (2009)
- [19] L.L. Sánchez-Sotoa, J.J. Monzóna, A.G. Barriusoa, J.F. Cariñenab, Phys. Rep. 513, 191 (2012)
- [20] I.I. Cotaescu, P. Gravila, M. Paulescu, Phys. Lett. A 366, 363 (2008)
- [21] N. Hatano, K. Sasada, H. Nakamura, T. Petrosky, Prog. Theor. Phys. 119, 187 (2007)
- [22] H. Ciftci, R.L. Hall, N. Saad, Phys. Lett. A 340, 388 (2005)
- [23] K. Ohta, R.E. Cohen, K. Hirose, K. Haule, K. Shimizu, Y. Ohishi, Phys. Rev. Lett. 108, 026403 (2012)
- [24] M. Abramowitz, I.A. Stegun, Handbook of Mathematical Functions with Formulas, Graphs, and Mathematical Tables (Dover Publications, Inc., New York, 1965)